

# Numerical Investigation of the Effect of Curvature and Reynold's Number to Radial Velocity in a Curved Porous Pipe

Mwangi DM<sup>1\*</sup>, Karanja S<sup>1</sup> and Kimathi M<sup>2</sup>

<sup>1</sup>Meru University of Science and Technology, Meru, Kenya

<sup>2</sup>Technical University of Kenya, Nairobi Kenya, Nairobi, Kenya

## Abstract

Different irrigation methods are being used in agriculture. However, due to scarcity of water, irrigation methods that use water efficiently are needed. The Motivation of this study is the increasing use of porous pipes to meet this requirement. The objective of this study is to investigate the effect of curvature and Reynold's number on radial velocity profile of water across a porous wall of a curved pipe with circular cross-section, constant permeability,  $k$  and porosity,  $\phi$ . The momentum equations of the two dimensional flow are written in toroidal coordinates. The main flow in the pipe is only characterized by  $\delta$  and  $Re$  as the only non-dimensional groups of numbers. We also considered the flow to be fully developed, unsteady, laminar and irrotational. Darcy law is used to analyse the flow across the porous membrane. The main flow was coupled with the flow through the porous wall of the pipe. The equations were solved using finite difference method. It was observed that effect of curvature on the velocity across the pipe wall is negligible while an increase in Reynold's number leads to an increase in the radial velocity. The findings of this study are important in the design of porous pipes and also in their use during irrigation.

**Keywords:** Unsteady; Incompressible; Curved; Porous; Coupling; Darcy law

## Nomenclature

Roman Symbol	Quantity
$t$	Time (s)
$u_r, u_\alpha, u_\theta$	Velocities of flow in the radial, circumferential and axial directions in the porous wall ( $\text{ms}^{-1}$ )
$v_r, v_\alpha, v_\theta$	Velocities of flow in the radial, circumferential and axial directions in the main pipe ( $\text{ms}^{-1}$ )
$\frac{\partial}{\partial r}, \frac{\partial}{\partial \alpha}, \frac{\partial}{\partial \theta}$	Derivatives in the radial, circumferential and axial directions
$r$	Distance measured from the center of the circular cross-section of the pipe
$a$	Inner cross-sectional radius
$R$	Radius of torus
$B$	$1 + \delta \cos \alpha$
$P$	Pressure ( $\text{Nm}^{-2}$ )
$\nabla$ Gradient operator	$\left( = i \frac{\partial}{\partial x} + j \frac{\partial}{\partial y} + k \frac{\partial}{\partial z} \right)$
$\nabla_2$ Laplacian operator	$\left( = \frac{\partial^2}{\partial x^2} + \frac{\partial^2}{\partial y^2} + \frac{\partial^2}{\partial z^2} \right)$
$g$	Acceleration due to gravity ( $\text{ms}^{-1}$ )
$Re$	Reynolds number (dimensionless)
$k$	Permeability ( $\text{m}^2$ )
$V$	Volume of void space ( $\text{m}_3$ )
$D$	Dean number (dimensionless)
$Da$	Darcy number (dimensionless)

$\rho$	Fluid density ( $\text{Kgm}^{-3}$ )
$\alpha$	Angle of fluid particle located in the cross-section of the pipe
$\theta$	Curvature angle of the pipe
$\delta$	Curvature ( $= a/R$ ) (dimensionless)
$\phi$	Porosity
$\mu$	Coefficient of viscosity ( $\text{Kgm}^{-1}\text{s}^{-1}$ )

## Introduction

In principle flow in a curved pipe can be described through the conservation laws: the conservation of mass, momentum and energy. The ratio of the inertia forces and the viscous forces acting on the fluid can be expressed in terms of the non-dimensional Reynolds number. However, due to the curvature of the pipe an additional force is added to the problem. This additional force is expressed through the non-dimensional curvature ratio  $\delta = \frac{a}{R}$  where  $a$  is the radius of pipe and  $R$  the centerline radius of the bent pipe. The Reynolds number and the curvature ratio yield the much used Dean number,  $De = Re\delta^{\frac{1}{2}}$ , where represents the Reynolds number and  $\delta$  the curvature ratio [1-10].

If a pipe is curved, the velocity profile will no longer be symmetrical about the axis of the pipe. Centrifugal force due to the change in direction of the flow sets up secondary currents in the plane of the cross-section, with the result that the maximum velocity is no longer

\*Corresponding author: Mwangi DM, Meru University of Science and Technology, Meru, Kenya, Tel: 254712524293; E-mail: [info@must.ac.ke](mailto:info@must.ac.ke)

Received July 31, 2017; Accepted August 02, 2017; Published August 17, 2017

Citation: Mwangi DM, Karanja S, Kimathi M (2017) Numerical Investigation of the Effect of Curvature and Reynold's Number to Radial Velocity in a Curved Porous Pipe. J Appl Computat Math 6: 363. doi: 10.4172/2168-9679.1000363

Copyright: © 2017 Mwangi DM, et al. This is an open-access article distributed under the terms of the Creative Commons Attribution License, which permits unrestricted use, distribution, and reproduction in any medium, provided the original author and source are credited.

at the center of the section but at some point intermediate between the center and the wall. No secondary flow is induced for an in viscid fluid since secondary flow is induced by centrifugal forces and their interaction primarily with viscous force [1]. The Dean number is a measure of the magnitude of the secondary flow. The curvature  $\delta$  is a more detailed measure of the effect of geometry and the extent to which the centrifugal force varies on the cross-section. Curvature affects the balance of inertia, viscous and centrifugal forces [11-15].

The centrifugal force ( $\frac{U^2}{R}$  where U is the velocity and R the radius of curvature) induced from the bend will act stronger on the fluid close to the pipe axis than close to the walls, since the higher velocity fluid is near the pipe axis. This gives rise to a secondary motion superposed on the primary flow, with the fluid in the center of the pipe being swept towards the outer side of the bend and the fluid near the pipe wall return towards the inside of the bend. The secondary motion appear as a pair of counter rotating cells widely known as Dean vortices Kalpakli [11], Dean [5] introduced the Dean number (D) a parameter that dynamically defines such flows and is named after him.

Fluid flow in a curved pipe has many applications to industrial fluid dynamics and physiological fluid flows. It has wide ranging applications to the design of heat exchangers, oil pipelines, chemical reaction plants and simulation of blood flow at curvature sites. The only additional parameter to the flow in a straight pipe is the curvature [16-23].

The first theoretical analysis of flow in a curved pipe was carried out by Dean [5] who presented the original analytical solution to the problem by assuming that the flow in a curved tube was in a steady, fully developed condition and that the secondary flow is just a small disturbance of the Poiseuille flow in a straight tube. A first order series solution was used to find this analytical solution. He compared his results with the experimental data obtained by Eustice [8], and found a good agreement. Dean's solution shows that the streamlines exhibit helical motion when the curvature of the pipe is small. In his first paper, Dean could not describe how the curvature of the pipe affects the flow near the boundary and the flow rate. In his second paper, Dean (1928), noticed that when the fluid motion is slow the reduction in flow rate due to curvature of the tube depends on the single variable k defined by  $k = \frac{2Re^2 a}{R}$ , where  $Re$  is the Reynolds number,  $a$  the radius of the tube and  $R$  the curvature radius of the tube. He derived a higher order series solution to describe the flow analytically in a tube with a small K- number. The approximation was valid up to  $K=576$ . He remarked that curvature reduces the pressure gradient on the boundary, so that the flux ratio decreases there.

Taylor [21] was able to show experimentally that steady stream-line motion persisted up to a Reynolds number, 5830, which is 2.8 times Reynolds' criterion for a straight pipe. He showed that for a curvature ratio of  $\delta = \frac{a}{R} = 0.0313$  the flow motion stays steady until  $Re=5010$ . Taylor's experiments were inspired by White [23] who investigated the streamlines of flow in curved tubes and noticed that turbulent flow through a curved tube exist but probably at a higher Reynolds numbers compared to a straight pipe. White was the first to use the 'Dean's criterion' term:  $\frac{\rho v d}{\mu} \sqrt{\frac{d}{D}} = Re \delta^{\frac{1}{2}}$  where  $\rho$  is the density,  $\mu$  the dynamic viscosity of the fluid,  $v$  the mean velocity,  $d$  the tube diameter,  $D$  the diameter of the curvature of the tube  $Re = \frac{\rho v d}{\mu}$  is the Reynold's number and  $\delta = \frac{d}{D}$  is the curvature.

Collins and Dennis [3] obtained numerical solutions for values of  $Dg$  upto 5000. They were able to show that as  $D$  increased the secondary motion causes an increasing displacement of the peak longitudinal velocity towards the outside of the bend. Berger [1] gave an extensive review of flow in rigid infinitely coiled pipes. Their primary concern was laminar incompressible flows. They gave the equations for the formulation of the problem of steady and laminar flow in a rigid pipe, fully developed flow and a brief outline on the analysis of unsteady flows.

There have been numerous recent studies in this area. Masud et al. [14] investigated incompressible viscous steady fluid flow through a curved pipe with circular cross-section under the combined effects of high Dean Numbers and a range of curvature,  $0.01 \leq \delta \leq 0.9$ .

Axial velocity was found to increase with increase of Dean Number and decrease with the increase of curvature. For high Dean Number and low curvature almost all the fluid particles leave the inner half of the cross-section. Two vortex solutions were found for secondary flow.

There has been numerous recent studies in this area. Masud et al. [14] investigated incompressible viscous steady fluid flow through a curved pipe with circular cross-section under the combined effects of high Dean Numbers and a range of curvature,  $0.01 \leq \delta \leq 0.9$ . Axial velocity was found to increase with increase of Dean Number and decrease with the increase of curvature. For high Dean Number and low curvature almost all the fluid particles leave the inner half of the cross-section. Two vortex solutions were found for secondary flow. Nobari and Amani [16] did a numerical investigation on developing flow and heat transfer in a curved pipe. Intensity of secondary flow was found to increase near the inlet and then decrease especially in the case on high dean numbers. Maximum friction factor and also maximum heat transfer rate also occurs in the entrance region. The maximum velocity location was found to shift from the centre to the outer wall of the curved pipe within the entrance region. The maximum axial velocity gets closer to the outer wall with increasing Reynolds number. The entrance length depends only on Reynolds number especially for  $\delta = \frac{1}{7}$ .

Hoque et al. [10] investigated the magneto hydrodynamics fluid flow through a curved pipe with circular cross-section under the combined effects of high Dean Number  $D$ , Magnetic parameter  $M_g$  and non-dimensional curvature  $\delta$ . The flow patterns were shown graphically for large dean numbers as well as magnetic parameter and a wide range of curvatures  $0.01 \leq \delta \leq 0.4$ . Two vortex solutions were found. Axial velocity was found to increase with the increase of Dean Number and decrease with the increase of curvature and magnetic parameter. For high magnetic parameter, Dean Number and low curvature almost all the fluid particles strength are weak.

Daneshfaraz [4] did a numerical investigation of velocity profile and pressure distribution of 3-D bends with different diversion angles via CFD model. Reynolds number's ranged from 100-900 and the diversion angles of bends were 90, 135, and 180 degrees with regard to inlet flow. The results showed that by increasing the section angle, the maximum velocity occurs at 0.7 to 0.9 of the pipe diameter from inner wall. By increasing the section angle, the pressure profile inclines to outer wall and in this inclination pressure loss is observed. For low Reynolds numbers, the variation of pressure loss is linear but by increasing the Reynolds number maximum pressure loss happens at limited section angle.

Park [17] made a numerical study of core-annular flow in a curved

pipe using the volume-of-fluid method. He investigated two cases: core-annular flow in a 90° bend and in a 180° return bend. He made a detailed analysis for the velocities and pressures occurring in a 90° bend and in a 180° return bend. The secondary flows were found to play an important role in the behavior of core-annular flow in a curved pipe. The demonstrated the skewness in the velocity profiles, toward the outer wall, as well as the structure of secondary flow patterns in curved tube geometries.

In our study, the wall of the curved pipe is porous. The capacity of a porous medium for allowing fluid to penetrate is given by hydraulic conductivity of the porous medium. It is denoted as the permeability,  $k$ . A characteristic property of porous media is the Porosity,  $\phi$ , which is a macroscopic property which rely on the permeability in a consolidated medium. It is defined as the ratio of the volume of the void space in the medium,  $v_{void}$  and the total volume of the medium,  $v_{total}$

$$\phi = \frac{V_{void}}{V_{total}} \phi \in [0, 1].$$

The flow in porous media can be categorized as either pre-Darcy flow, Darcy flow, Forchheimer flow or turbulent flow when the continuum approach is applied to the porous matrix. The demarcation parameter between the regions is the Reynolds number. According to Sobieski and Trykozko [20] most authors put the upper limit of the applicability of Darcy's law between  $Re=1$  and  $Re=10$  Darcy's law was formulated by Henry Darcy in 1856 based on his observations on the public water supply at Dijon and experiments on the steady-state unidirectional flow. It describes a linear relationship between flow rate and applied pressure. The law can also be derived from a spatial average of Stoke's equation.

$$u = \frac{Q}{A}$$

Where  $u$  is Darcy or filtration velocity defined as  $u = \frac{Q}{A}$  and  $k$  is the permeability.  $Q$  is the volumetric flow rate, and has units of ( $m^3/s$ ).  $A$  is the cross section of the porous media orthogonal to the flow. Darcy velocity,  $u$ , is related to the actual velocity,  $u$ , by the relation.

$$u = \phi u$$

Which means that Darcy velocity is smaller than actual velocity by a factor  $\phi$ .

Thus

$$\phi u = -\frac{k}{\mu} \nabla p$$

Darcy's law applies only to the cases where the flow through pores of a porous medium can be modeled as stokes flow. The law forms a basis for modeling fluid transport in porous media. In applications where fluid velocities are low, Darcy's law well describes the fluid transport in porous media but where the fluid velocities are high, the fluid transport predicted by Darcy's law usually departs from measurements considerably.

While the idea of using porous materials in irrigation by burying clay pots near the roots or, later using clay pipes, is very old, a pioneer paper on the subject of use of porous pipes in irrigation which described use of canvas hoses to deliver water to the ground was by Robey [19]. Fasano and Farina [9] mentions more recent technical studies in this area and also appreciates that this technique is today used to such a large extent that periodic international conferences are held.

Porous flow dates back to 1856 when Darcy described empirically the relation between the hydraulic gradient,  $I$ , and the discharge

velocity,  $v$ , through porous sands and sandstones as  $V=Ki$  where  $k$  is the permeability coefficient (m/s). These expressions have later been referred to as the Darcy law. It applies to the laminar flow case without convective inertia forces i.e., creeping flow.

Labecki et al. [13] developed a model in which the lumen and shell sides of a fibre bundle are treated as two interpenetrating porous regions. Darcy's law and fluid continuity were combined to give a set of two dimensional partial differential equations governing the hydrodynamics within hollow-fibre membrane devices. The computational domain corresponded to the real dimensions of a hollow-fibre cartridge and hence macroscopic radial gradients, which exist during some operations, could be taken into account. Effects of fibre expansion under wet conditions were included. Closed shell mode, dead end and cross-flow filtration as well as counter-current and co-current contacting configurations were analysed. The effects of the membrane and shell-side hydraulic permeabilities on the volumetric flow rates and spatial flow distribution were investigated and the predictions were compared with those of one-dimensional models based on the Krogh cylinder approximation.

Erdoğan and Imrak [7] theoretically considered a fully developed laminar flow of an incompressible viscous fluid through a porous pipe with suction and injection. They gave an exact solution of the Navier-Stokes equation. Their study found that the flow properties depend on the cross-Reynolds number. For large values of the cross-Reynolds number, the flow near the region of the suction shows a boundary layer character. The velocity and vorticity vary sharply in this region. Outside the boundary layer, the velocity and the vorticity do not show an appreciable change.

Brown and Lai [2] conducted experiments to measure the permeability and slip coefficient of seven porous tubes made from fiberglass and nylon nettings with various wall thicknesses. Permeability's in both the longitudinal and radial directions were found to depend on the material but the radial permeability also depends on wall thickness. The slip coefficient was found to depend on the material, Reynolds number, permeabilities and wall thickness.

Nabotavi et al. [15] simulated fluid flow in three-dimensional random fibrous media using the lattice Boltzman method. They determined the permeability of the medium using the Darcy law across a wide range of void fractions ( $0.08 \leq k \leq 0.99$ ) and found that the values for the permeability that they obtained were consistent with available experimental data. They used the numerical data to develop a semi-empirical constitutive model for the permeability of fibrous media as a function of their porosity and of the fibre diameter. They performed further simulations to determine the impact of the curvature and aspect ratio (length to diameter ratio of straight cylindrical fibres of finite length) of the fibres on the permeability and found that curvature has a negligible effect, and that aspect ratio is only important for fibres with aspect ratio smaller than 6:1, in which case the permeability increases with increasing aspect ratio. They finally numerically calculated the permeability tensor for the fibrous media studied and confirmed that, for an isotropic medium, the permeability tensor reduces to a scalar value.

Fasano and Farina [9] in their study that sought to design irrigation pipes applied the fundamental laws of dynamics of fluids in a pipe (Navier stokes equations) and through porous media (Darcy's law) in incompressible laminar flow through hollow fibers with porous walls in a dead end configuration. One of the key points was to obtain at the far end of the pipe a water delivery rate similar to the one close to the inlet. They exploited the smallness of the ratio  $\epsilon$  between the

radius and the length of the pipe to expand all the relevant quantities in power of  $\epsilon$  in the upscaling procedure. They coupled the flow in the pipe and the flow across the wall by use of the boundary conditions in the inner wall. The velocity profiles for the longitudinal and for the cross-flow were analytically determined. The explicit expression of the permeability of the system was then determined.

From the literature flows in curved pipes have mainly been characterized by dean number and curvature ratio and also Wimberley number in case of pulsate flows. The dean number,  $D = Re\delta^{\frac{1}{2}}$ , combines both  $Re$  and  $\delta$  such that the effect of  $\delta$  on flow cannot be independently determined. Furthermore, none of these studies has coupled the flow in a curved pipe with the flow through the porous wall of the pipe for an unsteady and irrotational flow using numerical methods. This study is going to couple the flow in a curved pipe and the flow through the pipe's porous wall in determining the effect of curvature,  $\delta(0,1)$ , and the effect of Reynold's number on velocity through the porous wall of a pipe with cylindrical cross-section using numerical methods for an unsteady, irrotational and incompressible flow.

## Governing Equations

### Equation of continuity

The equation of continuity (mass conservation equation) is derived from the law of conservation of mass. If a given fluid mass is followed as it flows its mass will remain unchanged if no nuclear reactions are taking place. The continuity equation for an incompressible fluid in the pipe is given by

$$\frac{\partial \rho}{\partial t} + \frac{\partial}{\partial (x_i)} (u_i) = 0$$

Where  $i=1,2,3$  along the  $x$ ,  $y$  and  $z$  directions respectively. For a curved pipe the equation was written in toroidal coordinates. The curved pipe would form a torus with a radius  $R$  and toroidal coordinates  $(r, \alpha, \theta)$ . The toroidal coordinate system belongs to the orthogonal curvilinear coordinates group. The continuity equation has been derived in toroidal coordinates from the Navier-Stokes equation in Verkaik [22] following orthogonal curvilinear coordinates (Figure 1).

The distance covered by a fluid particle from the entry point into the torus When  $\theta=0$  is given by  $R\theta$ . The continuity equation in toroidal coordinates becomes

$$\frac{\partial v_r}{\partial r} + \frac{v_r}{r} + \frac{1}{r} \frac{\partial v_\alpha}{\partial \alpha} + \frac{1}{R + r \cos \alpha} \frac{\partial v_\theta}{\partial \theta} + \frac{v_r \cos \alpha - v_\alpha \sin \alpha}{R + r \cos \alpha} = 0 \quad (1)$$

Where  $V_r$ ,  $V_\alpha$  and  $V_\theta$  are the velocities in the radial, circumferential and axial direction respectively in the main pipe  $\theta$  is curvature angle of the curved pipe and  $\alpha$  is the angle of a liquid particle located in the cross-section of the pipe.

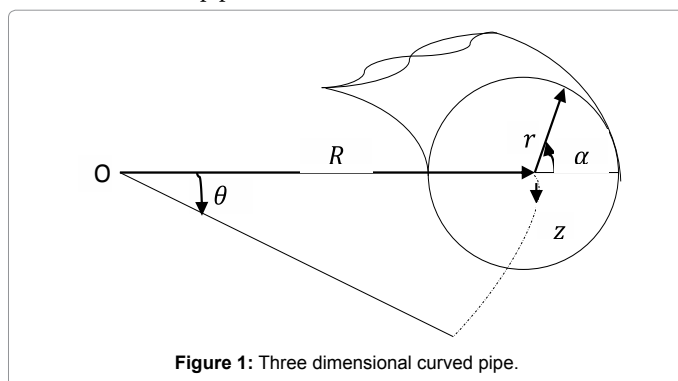


Figure 1: Three dimensional curved pipe.

The continuity equation across the porous wall will be written in cylindrical coordinates

$$\frac{\partial u_r}{\partial r} + \frac{u_r}{r} + \frac{1}{r} \frac{\partial u_\alpha}{\partial \alpha} + \frac{\partial u_\theta}{\partial \theta} = 0 \quad (2)$$

### Equation of momentum

The principle of conservation of momentum applies Newton's law of motion to an element of the fluid. Newton's second law of motion states that the rate of change of momentum of a body is equal to the resultant forces acting on the body. The external forces that act on the fluid are either body forces that act at a distance on a fluid particle or surface forces due to direct contact of a fluid with other fluid particles or walls of the boundary. The Navier-Stokes equation momentum equation is given in tensor form as

$$\rho \frac{\partial u_j}{\partial t} + \rho u_k \frac{\partial u_j}{\partial x_k} = \frac{\partial \sigma_{ij}}{\partial x_i} + \rho f_j$$

The terms  $\rho \frac{\partial u_j}{\partial t}$  and  $\rho u_k \frac{\partial u_j}{\partial x_k}$  give the local acceleration and convective acceleration respectively. The local acceleration represents the change in velocity with time at any point in space while the convective acceleration represents the change in velocity due to the fact that a given fluid element changes position with time and therefore assumes different values of velocity as it flows even in steady flows. The terms  $\frac{\partial \sigma_{ij}}{\partial x_i}$  and  $\rho f_j$  are the forces due to surface shear stress and due to body forces respectively. The body forces that act on the fluid under consideration are force due to gravity and centrifugal force due to curvature of the pipe, Masud et al. [14].

The derivation has been shown in Verkaik [22]. The equations are:

#### Radial Momentum

$$\frac{\partial v_r}{\partial t} + v_r \frac{\partial v_r}{\partial r} + \frac{v_\alpha}{r} \frac{\partial v_r}{\partial \alpha} - \frac{v_\alpha^2}{r} - \frac{v_\theta^2 \cos \alpha}{R + r \cos \alpha} + \frac{v_\theta}{R + r \cos \alpha} \frac{\partial v_r}{\partial \theta} = -\frac{1}{\rho} \frac{\partial p}{\partial r} + v \left\{ \frac{\partial^2 v_r}{\partial r^2} + \frac{1}{r} \frac{\partial v_r}{\partial r} - \frac{v_r}{r^2} + \frac{1}{r^2} \frac{\partial^2 v_r}{\partial \alpha^2} - \frac{2}{r^2} \frac{\partial v_\alpha}{\partial \alpha} + \frac{1}{(R + r \cos \alpha)^2} \frac{\partial^2 v_r}{\partial \theta^2} \right\} + v \left\{ \frac{1}{R + r \cos \alpha} \left[ \cos \alpha \frac{\partial v_r}{\partial r} - \frac{\sin \alpha}{r} \frac{\partial v_r}{\partial \alpha} + \frac{v_\alpha \sin \alpha}{r} \right] + \frac{2 \sin \alpha}{(R + r \cos \alpha)^2} \frac{\partial v_\theta}{\partial \theta} - \frac{\cos \alpha}{(R + r \cos \alpha)^2} [v_r \cos \alpha - v_\alpha \sin \alpha] \right\} \quad (3)$$

#### Axial momentum

$$\frac{\partial v_\theta}{\partial t} + v_r \frac{\partial v_\theta}{\partial r} + \frac{v_\alpha}{r} \frac{\partial v_\theta}{\partial \alpha} + \frac{v_\theta}{R + r \cos \alpha} \frac{\partial v_\theta}{\partial \theta} + \frac{v_\alpha (v_r \cos \alpha - v_\alpha \sin \alpha)}{R + r \cos \alpha} = \frac{1}{\rho} \frac{R}{R + r \cos \alpha} \frac{\partial p}{\partial \theta} + v \left\{ \frac{\partial^2 v_\theta}{\partial r^2} + \frac{1}{r} \frac{\partial v_\theta}{\partial r} + \frac{1}{r^2} \frac{\partial^2 v_\theta}{\partial \alpha^2} - \frac{v_\theta}{(R + r \cos \alpha)^2} \frac{\partial^2 v_\theta}{\partial \theta^2} - \frac{v_\theta}{(R + r \cos \alpha)^2} \right\} + v \left\{ \frac{1}{r} \frac{\partial v_\theta}{\partial r} + \frac{1}{R + r \cos \alpha} \left[ \cos \alpha \frac{\partial v_\theta}{\partial r} - \frac{\sin \alpha}{r} \frac{\partial v_\theta}{\partial \alpha} \right] + \frac{2}{(R + r \cos \alpha)^2} \left[ \cos \alpha \frac{\partial v_r}{\partial \theta} - \sin \alpha \frac{\partial v_\alpha}{\partial \theta} \right] \right\} \quad (4)$$

#### Circumferential momentum

$$\frac{\partial v_\alpha}{\partial t} + v_r \frac{\partial v_\alpha}{\partial r} + \frac{v_\alpha}{r} \frac{\partial v_\alpha}{\partial \alpha} + \frac{v_r v_\alpha}{r} + \frac{v_\theta}{R + r \cos \alpha} \frac{\partial v_\alpha}{\partial \theta} + \frac{v_\theta^2 \sin \alpha}{R + r \cos \alpha} = \frac{1}{\rho} \frac{\partial p}{\partial \alpha} + v \left\{ \frac{\partial^2 v_\alpha}{\partial r^2} + \frac{1}{r} \frac{\partial v_\alpha}{\partial r} - \frac{v_\alpha}{r^2} + \frac{1}{r^2} \frac{\partial^2 v_\alpha}{\partial \alpha^2} - \frac{2}{r^2} \frac{\partial v_r}{\partial \alpha} + \frac{1}{(R + r \cos \alpha)^2} \frac{\partial^2 v_\alpha}{\partial \theta^2} \right\} + v \left\{ \frac{\cos \alpha}{(R + r \cos \alpha)^2} \frac{\partial v_\alpha}{\partial r} - \frac{\sin \alpha}{R + r \cos \alpha} \left[ \frac{1}{r} \frac{\partial v_\alpha}{\partial \alpha} + \frac{v_r}{r} \right] + \frac{2 \sin \alpha}{(R + r \cos \alpha)^2} \frac{\partial v_\theta}{\partial \theta} \right\} + v \left\{ \frac{\sin \alpha}{(R + r \cos \alpha)^2} [v_r \cos \alpha - v_\alpha \sin \alpha] \right\} \quad (5)$$

### Darcy law

The Darcy law governs the flow through the porous wall. It describes a linear relationship between flow rate and applied pressure. In vectoral form, this relation reads as

$$(\mathbf{u})_s = \frac{k}{\mu} \nabla(p)_i$$

Where  $(u)_s$  is the superficial velocity through the porous wall,  $\nabla p$  the applied intrinsic pressure gradient and  $k$  is the permeability which can be experimentally determined by applying a constant pressure gradient and measuring the flow rate  $Q=A.(u)_s$  through a given cross sectional area. The superficial velocity is related to the intrinsic velocity by  $(u)_s = \phi(u)_i$ . The equation can be rewritten as

$$\phi(\mathbf{u})_i = \frac{k}{\mu} \nabla(p)_i \tag{6}$$

The Darcy or creeping flow regime is valid for the Reynolds number  $Re < 10$ , Khayamyan and Lundstrom [12], where  $Re$  is based on pore diameter i.e.,

$$Re = \frac{\rho d v}{\mu}$$

### Mathematical Model

#### Approximations and assumptions

For an irrational flow, the velocity in the circumferential direction equals zero ( $V_\alpha=0$ ), the momentum equation and all derivatives in  $\alpha$ -direction ( $\frac{\partial}{\partial \alpha} = 0$ ) will be omitted. The coordinates will reduce to only axial and radial. For a fully developed flow all derivatives in  $\theta$  direction are zero ( $\frac{\partial}{\partial \theta} = 0$ ). This does not hold for the driving force  $\frac{\partial p}{\partial \theta}$ .

Equation (5) reduces to zero while eqns. (1-4) reduces to (7-10), respectively as shown below continuity equation in the main pipe.

$$\frac{\partial v_r}{\partial r} + \frac{v_r}{r} + \frac{v_r \cos \alpha}{R + r \cos \alpha} = 0 \tag{7}$$

Continuity equation in the pipe wall

$$\frac{\partial u_r}{\partial r} + \frac{u_r}{r} = 0 \tag{8}$$

The momentum equations reduces to

Radial momentum

$$\begin{aligned} \frac{\partial v_r}{\partial t} + v_r \frac{\partial v_r}{\partial r} - \frac{v_\theta^2 \cos \alpha}{R + r \cos \alpha} = -\frac{1}{\rho} \frac{\partial p}{\partial r} + \nu \left\{ \frac{\partial^2 v_r}{\partial r^2} + \frac{1}{r} \frac{\partial v_r}{\partial r} - \frac{v_r}{r^2} \right\} + \\ \nu \left\{ \frac{1}{R + r \cos \alpha} \left[ \cos \alpha \frac{\partial v_r}{\partial r} \right] - \frac{\cos \alpha}{(R + r \cos \alpha)^2} [v_r \cos \alpha] \right\} \end{aligned} \tag{9}$$

Axial momentum

$$\begin{aligned} \frac{\partial v_\theta}{\partial t} + v_r \frac{\partial v_\theta}{\partial r} + \frac{v_\theta v_r \cos \alpha}{R + r \cos \alpha} = \frac{1}{\rho} \frac{R}{R + r \cos \alpha} \frac{\partial p}{\partial \theta} + \nu \left\{ \frac{\partial^2 v_\theta}{\partial r^2} - \frac{v_\theta}{(R + r \cos \alpha)^2} \right\} + \\ \nu \left\{ \frac{1}{r} \frac{\partial v_\theta}{\partial r} + \frac{1}{R + r \cos \alpha} \cos \alpha \frac{\partial v_\theta}{\partial r} \right\} \end{aligned} \tag{10}$$

### Scaling variables

In this study the non-dimensionalisation process is based on the following sets of scaling variables and the non-dimensional parameters.

$$r^* = \frac{r}{a}, \quad t^* = \frac{U t}{a}, \quad u_r^* = \frac{u_r}{U}, \quad v_r^* = \frac{v_r}{U}, \quad v_\theta^* = \frac{v_\theta}{U}, \quad p^* = \frac{p}{\rho U^2} \tag{11}$$

Where the asterisk represents the dimensionless quantities.

### Non-dimensionalisation

Non-dimensionalisation allows us to reduce the number of variables that affect a given physical phenomena. The motivation of the transformation into dimensionless form is to make generalization of the results of either theoretical or experimental investigations possible and also to enable modeling by using similarity criteria that determine the actual conditions of the problem. If the non-dimensional parameters are the same for two geometrically similar situations, then the equations of the non-dimensional variables are the same. Hence, they have the same solutions and the same flow patterns. We use the scaling variables given above and non-dimensional parameters to non-dimensionalise the equations governing the flow.

Continuity equation

$$\frac{\partial v_r}{\partial r} + \frac{v_r}{r} + \frac{\delta v_r \cos \alpha}{1 + \delta r \cos \alpha} = 0$$

Which can also be written as

$$\frac{\partial}{\partial r} (r B v_r) = 0 \tag{12}$$

Where  $B = 1 + \delta r \cos \alpha$

Radial momentum equation

$$\begin{aligned} \frac{\partial v_r}{\partial t} + v_r \frac{\partial v_r}{\partial r} - \frac{\delta v_\theta^2 \cos \alpha}{B} = \\ -\frac{\partial p}{\partial r} + \frac{1}{Re} \left\{ \frac{\partial^2 v_r}{\partial r^2} + \frac{1}{r} \frac{\partial v_r}{\partial r} - \frac{v_r}{r^2} + \frac{\delta}{B} \cos \alpha \frac{\partial v_r}{\partial r} - \frac{\delta^2 \cos \alpha}{B^2} v_r \cos \alpha \right\} \end{aligned}$$

Since

$$v_r \frac{\partial v_r}{\partial r} + \frac{\delta v_r^2 \cos \alpha}{B} + \frac{v_r^2}{r} = 0$$

The equation can also be written as

$$\begin{aligned} \frac{\partial v_r}{\partial t} + \frac{1}{r B} \left[ \frac{\partial}{\partial r} (r B v_r^2) - \delta r \cos \alpha v_\theta^2 \right] = \\ -\frac{\partial p}{\partial r} + \frac{1}{Re} \left[ \frac{1}{r B} \left\{ \frac{\partial}{\partial r} \left( r B \frac{\partial v_r}{\partial r} \right) \right\} - \frac{v_r}{r^2} - \frac{\delta^2 \cos \alpha}{B^2} v_r \cos \alpha \right] \end{aligned} \tag{13}$$

Axial momentum equation

$$\begin{aligned} \frac{\partial v_\theta}{\partial t} + v_r \frac{\partial v_\theta}{\partial r} + \frac{\delta v_\theta v_r \cos \alpha}{B} = \frac{\delta}{B} \frac{\partial p}{\partial \theta} + \\ \frac{1}{Re} \left\{ \frac{\partial^2 v_\theta}{\partial r^2} - \frac{\delta^2 v_\theta}{B^2} + \frac{1}{r} \frac{\partial v_\theta}{\partial r} + \frac{\delta}{B} \cos \alpha \frac{\partial v_\theta}{\partial r} \right\} \end{aligned}$$

Since

$$v_\theta \frac{\partial v_r}{\partial r} + \frac{v_\theta v_r}{r} + \frac{\delta v_\theta v_r \cos \alpha}{B} = 0$$

The equation can also be written as

$$\begin{aligned} \frac{\partial v_\theta}{\partial t} + \frac{1}{r B} \left[ \frac{\partial}{\partial r} (r B v_r v_\theta) + \delta r v_r v_\theta \cos \alpha \right] = \\ -\frac{\delta}{B} \frac{\partial p}{\partial \theta} + \frac{1}{Re} \left[ \frac{1}{r B} \left\{ \frac{\partial}{\partial r} \left( r B \frac{\partial v_\theta}{\partial r} \right) \right\} - \frac{\delta^2 v_\theta}{B^2} \right] \end{aligned} \tag{14}$$

To simplify the problem further the assumption that the pressure is constant over a cross-section because of comparatively small radial component of flow is made  $\frac{\partial p}{\partial \theta}$  is independent of  $\theta$  hence a constant.

Assuming that the flow along the pipe is symmetrical, then, in the plane of symmetry  $\alpha=0, \pi$  and,  $\cos \alpha = \pm 1$ . Taking the positive cosine we have

$$\frac{\partial v_r}{\partial t} + \frac{1}{rB} \left[ \frac{\partial}{\partial r} (rBv_r^2) - \delta r v_\theta^2 \right] = -A + \frac{1}{Re} \left\{ \frac{\partial^2 v_r}{\partial r^2} + \frac{1}{r} \frac{\partial v_r}{\partial r} - \frac{v_r}{r^2} + \frac{\delta}{B} \frac{\partial v_r}{\partial r} - \frac{\delta^2 v_r}{B^2} \right\} \quad (15)$$

$$\frac{\partial v_\theta}{\partial t} + \frac{1}{rB} \left[ \frac{\partial}{\partial r} (rBv_r v_\theta) + \delta r v_r v_\theta \right] = -\frac{\delta}{B} D + \frac{1}{Re} \left\{ \frac{\partial^2 v_\theta}{\partial r^2} + \frac{1}{r} \frac{\partial v_\theta}{\partial r} + \frac{\delta}{B} \frac{\partial v_\theta}{\partial r} - \frac{\delta^2 v_\theta}{B^2} \right\} \quad (16)$$

From our assumption of fully developed flow  $V_\theta$  is a constant hence only the momentum eqn. (15) will be solved.

### Flow through the porous wall

The seeping water flows radially through the porous pipe. The water that radially gets to the inner pipe wall then flows through the pores that open up in the outer wall. We are going to use boundary conditions to connect the flow in the main pipe and the flow through the porous wall i.e., at the inner boundary  $u_r = \phi v_r$ .

The centerline of the pipe is assumed to lie on the arc of a circle of radius  $N$  so that torsion effects are neglected. The flow is assumed to be symmetrical about the center line, the porous material is considered homogenous and isotropic and there is no buildup of particles on the surface or within the porous wall (Figure 2).

We non-dimensionalise the Darcy law by taking  $Da = \frac{k}{a^2}$  and  $Re = \frac{\rho a U}{\mu}$  to get

$$u_r = -DaRe \frac{1}{\phi} \frac{\partial p_m}{\partial r} \quad (17)$$

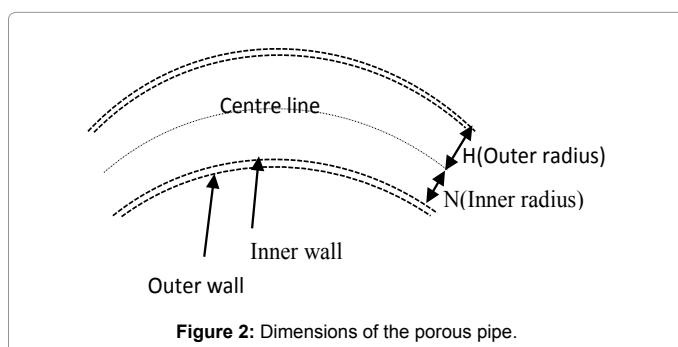
### Equation of pressure

From Darcy's law, there is a linear relationship between pressure and velocity. Substituting eqn. (17) in continuity equation (8) we get

$$\frac{\partial}{\partial r} \left( -DaRe \frac{1}{\phi} \frac{\partial p_m}{\partial r} \right) + \frac{1}{r} \left( -DaRe \frac{1}{\phi} \frac{\partial p_m}{\partial r} \right) = 0$$

Rearranging

$$\frac{\partial^2 p_m}{\partial r^2} + \frac{1}{r} \frac{\partial p_m}{\partial r} = 0 \quad (18)$$



Eqn. (18) was used in solving eqn. (17).

## Results and Discussion

Unsteady laminar flow for viscous incompressible fluid (water) has been numerically analyzed under low pressure gradient force for a range of curvature and Reynold's number. The method of finite differences has been used.

### Radial velocity in the main pipe with varying curvature

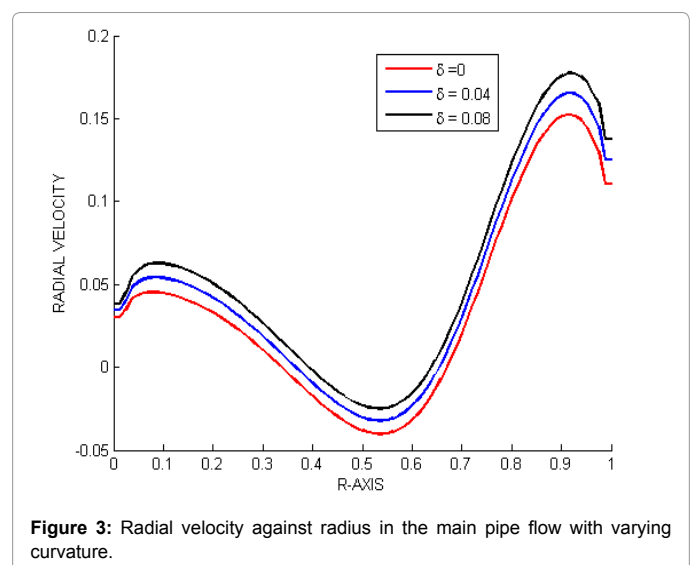
In solving eqn. (15) the pressure and axial velocity of the flow were held constant with pressure  $A=-0.18$  and axial velocity  $v_\theta=1$ . The values of radial velocity  $v_r$  were plotted against radius  $0 \leq r \leq 1$  for varying curvature ratio  $\delta$ . The graph shown in Figure 3 was obtained.

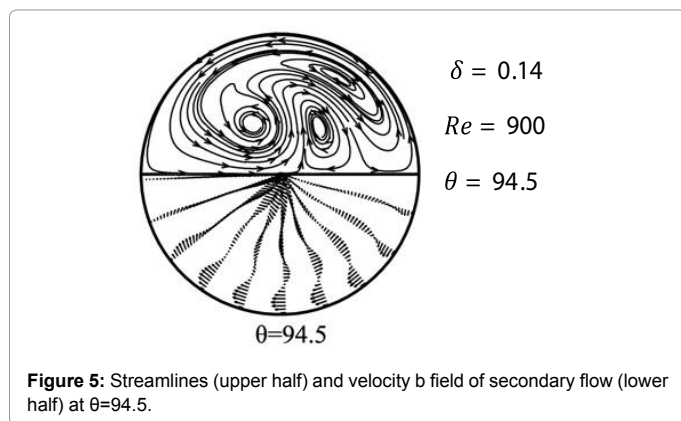
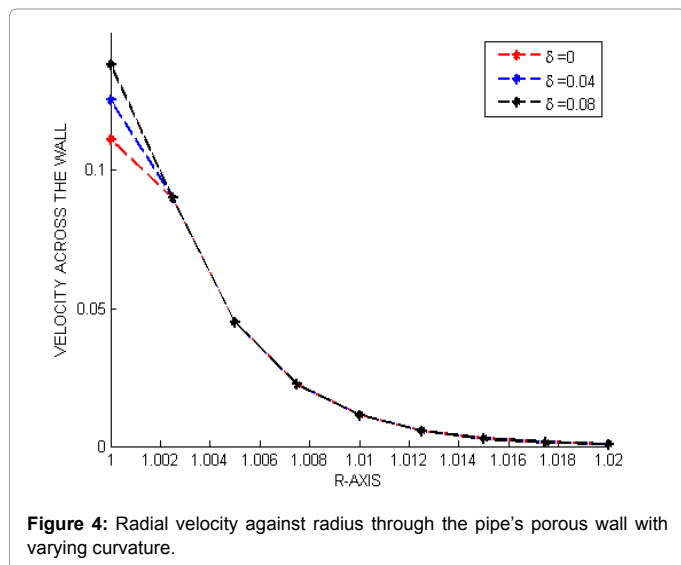
In Figure 3, positive values for the radial velocity mean a flow direction towards the center while negative values mean a flow direction away from the center towards the wall. The flow is forced outwards in a large region near the center and moves inwards in a small region near the wall. This secondary flow which is perpendicular to the mean flow is due to the pipe's curvature which induces a centrifugal force proportional to the flow speed squared. Thus, the flow is accelerated outwards near the center where its speed is high and inwards where the speed is low due to fulfillment of continuity.

Notice that due to the porosity of the wall the velocity does not go to zero at the inner wall. Since the continuity equation has to be fulfilled, and the mass flow out through the porous wall is small, the flow velocity is high in the small area where it moves inwards. From the Figure 3 the velocity profiles are similar for different curvature ratios. Although the velocity profiles are similar, an increase in curvature leads to an increase in radial velocity in the main pipe flow (Figure 4).

Nobari and Amani (2009) obtained streamlines and velocity field at different Sections, Reynolds's number and curvature ratios. We consider their results at the section  $\theta=94.5$  as shown in Figure 5 to be fully developed and compare with our results. Like in our study,  $\theta$  in this study is the axial direction. The length of the vectors is proportional to the magnitude of the flow. These results compare favorably with our findings.

Our results compare well with the study by Park [17] about single phase flow in  $90^\circ$  bend at different cross-sections of a pipe for different





Reynolds numbers at  $\alpha=90^\circ$ . The radial velocity profile is similar to our results the only difference being the velocity at the wall. The radial velocity at the wall in Park's study goes to zero because the pipe was not porous. In our case the wall is porous hence the radial velocity at the inner pipe wall is non-zero due to continuity.

### Radial velocity through the porous wall of the pipe with varying curvature

In solving eqn. (17) the flow through the porous wall is coupled with the flow in the main pipe. The constants used in the equation were Darcy number  $Da=10^{-7}$ , porosity  $\phi=0.4$  and porous membrane pressure  $p_m=-0.18$ .

We used the velocities at the inner pipe wall which marks the boundary between the main flow and the porous media flow as the initial conditions for the radial velocity through the porous pipe wall  $u_r$  i.e., the velocity at  $r=1$  in Figure 3 become starting velocity for the flow through the porous wall in Figure 4. Different curvature ratios were used for the same Reynolds's number and the results recorded in a graph as shown in Figure 4.

We have already seen that higher curvature values are associated with higher radial velocities in the main pipe flow from Figure 3. However, this is not the case in the porous medium. The results in Figure 4 show that for different boundary conditions at the inner pipe wall, the

velocity profiles for different values of curvature are seen to converge after a very short distance from the inner wall. This means that again, the flow through the porous wall was coupled with the flow in the main pipe. To achieve this, eqn. (17) were solved boundary conditions at the inner pipe wall have a negligible effect on the magnitude of velocity through the porous wall. Curvature ratio affects the flow in the main pipe, but negligibly so in the porous wall.

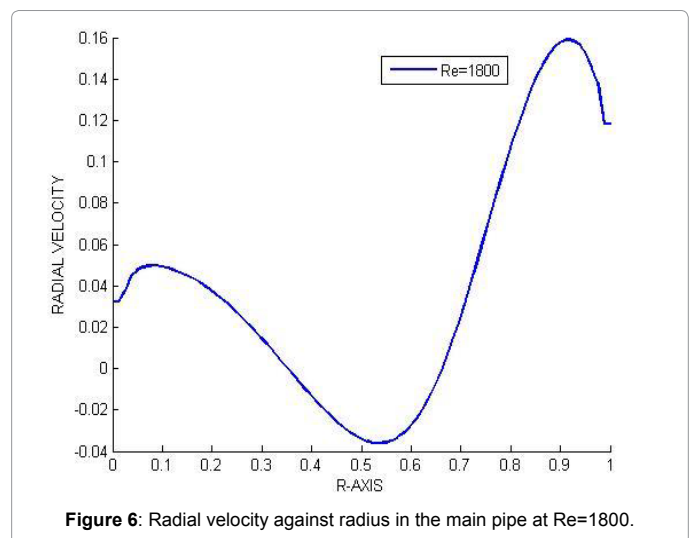
The findings of Nabotavi [15] allow us to hold  $Da$  constant for varying curvature values as we have done in our study. He showed that the effect of curvature on permeability of a fiber in a fibrous medium has no effect on the overall permeability of the medium by replacing straight fibers with randomly curved fibers as the constituting elements of porous medium.

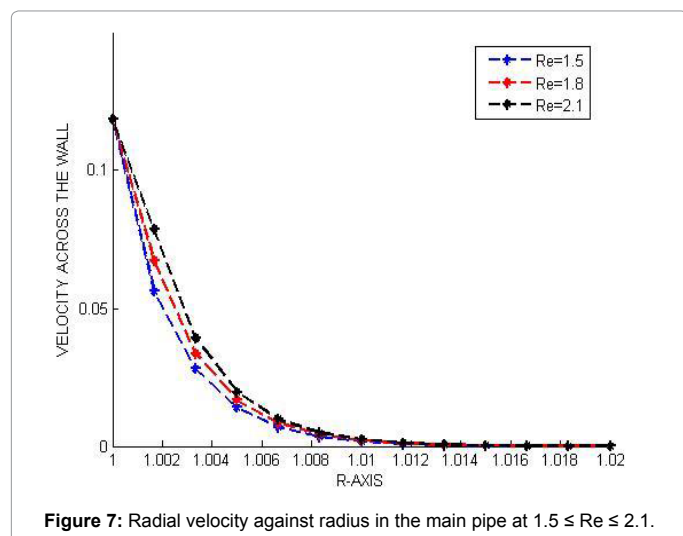
### Radial velocity through the porous wall of the pipe with varying Reynolds's number

The Reynold's numbers in the two flow regimes i.e., the Navier-Stokes flow in the main flow of the pipe and the Darcy flow through the pipe's wall are chosen differently. First eqn. (15) was solved by choosing  $Re=1800$  and constant curvature ratio. At the chosen  $Re$ , the flow is still well within the laminar range. The other constants used were as in (a). Again, the flow through the porous wall was coupled with the flow in the main pipe. To achieve this, equation (17) was solved with the  $Re$  being varied. The constants used were as in (b). We used the velocity at the inner pipe wall which marks the boundary between the main flow and the porous media flow as the initial condition for the radial velocity through the porous pipe wall  $u_r$  i.e., the velocity at  $r=1$  in Figure 6 become starting velocity for the flow through the porous wall in Figure 7. The results were recorded in a graph as shown in Figure 7.

The velocity profiles for the different  $Re$  in the porous medium are similar in shape but different in magnitude. The velocities decrease sharply from the inner pipe wall within a very short distance into the wall and then decreases gradually to near zero further away from the inner pipe wall towards the outer wall. In the porous wall the radius of the pores in the pore scale have very small radius. The no slip condition is obeyed at the wall of the fiber (if we view the pores as a network of fibers, each opening from the inner wall to the outer wall).

The velocity of a fluid increases with distance from the walls of the pipe. If the radius of the pipe is very small like the radius of the pore in the pore scale the maximum velocity attained will also be small.





This explains the drastic reduction in velocity from the inner pipe wall to the outer one. In other words, viscous forces are dominant in the flow through the porous wall, due to the small diameter of the pores hence the reduction in the velocity. At a higher  $Re$  the velocity through the porous wall is also higher. If we take the difference in  $Re$  in the porous medium to be due to difference in the pore radius, then, the flow velocity is higher in the flow with a higher  $Re$  through the porous medium.

From the results we were able to look at the effect of  $Re$  and  $\delta$  in a curved pipe independently of each other as opposed to most studies where the two parameters are combined together in the Dean number. We have gone ahead and coupled the flow in the main pipe and its porous wall by use of the wall boundary conditions and looked at the effect of the two parameters on the flow through the porous wall of a curved pipe.

## Conclusions

The objective of this study was to determine the effect of curvature and Reynolds number on the radial velocity in a curved porous pipe and also come up with equation of pressure. Coming up with the equation of pressure across the porous wall was a necessary step in obtaining radial velocity profile across the porous wall. The equation was obtained by using the linear relationship between velocity and pressure as given in Darcy and the continuity equation. In determining the effect of curvature and the Reynolds number, we coupled the equations of flow in the main pipe and the porous wall. Due to continuity, the velocity at the inner pipe wall became the velocity boundary condition for the flow through the porous wall.

From the velocity profiles obtained, the following conclusions are drawn:

1. Increase in curvature ratio leads to increase in radial velocity in the main pipe
2. Variation of curvature has negligible effect on the radial velocity through the porous wall. Taking this finding to porous pipe irrigation, it means that even if the porous pipe being used needs to be curved depending on the orientation of the crops on the ground, the crops lying along a straight and those lying along the curve will be watered uniformly.
3. An increase in Reynolds's number in the porous media leads to increase in radial velocity across the wall of the porous pipe

for the same initial condition at the inner pipe wall. In the case of water used during irrigation, it means that if we hold the density, viscosity and radius of the main pipe constant, an increase in  $Re$  in the porous medium lead to higher velocity through the porous wall which in turn leads to higher volume of water wetting the soil. Less time would then be required to wet the soil with a specified volume of water when  $Re$  is high as compared to when it is low.

## References

1. Berger SA, Talbot L, Yao LS (1983) Flow in Curved Pipes. Annual Review of Fluid Mechanics 15: 461-512.
2. Brown NM, Lai FC. (2006) Measurement of permeability and slip coefficient of porous tubes. Journal of Fluids Engineering 128: 987-992.
3. Collins WM, Dennis SCR (1975) The steady motion of a viscous fluid in a curved tube. Quarterly Journal of Mechanics and Applied Mathematics 28: 133-156.
4. Daneshfaraz R (2013) 3-D Investigation of velocity profile and pressure distribution in bends with different diversion angle. Journal of Civil Engineering and Science 2: 234-240.
5. Dean WR (1927) Note on the motion of fluid in a curved pipe. Philosophical Magazine 4: 208-222.
6. Dean WR (1928) The stream-line motion of fluid in a curved pipe. Philosophical Magazine S3: 673-695.
7. Erdoğlan ME, Imrak CE (2005) On the axial flow of an incompressible viscous fluid in a pipe with a porous boundary. Acta Mechanica 178: 187-197.
8. Eustice J (1911) Experiments of streamline motion in curved pipes. Proceedings of the Royal Society London Series A 85: 199-131.
9. Fasano A, Farina A (2011) Designing irrigation pipes. Journal of Mathematics in Industry 1: 1-19.
10. Hoque M, Anika NS, Alam M (2013) Numerical analysis of magnetohydrodynamics flow in a curved duct. International Journal of Scientific and Engineering Research 7: 607-617.
11. Kalpakli A (2012) Experimental study of turbulent flows through pipe bends. Technical reports from Royal Institute of Technology KTH Mechanics.
12. Khayamyan S, Lundstrom TS (2015). Interaction between the flow in two nearby pores within a porous material during transitional and turbulent flow. Journal of Applied Fluid Mechanics 2: 281-290.
13. Labecki M, Piret JM, Bowen BD (1995) Two-Dimensional analysis of fluid-flow in hollow fiber modules. Chemical Engineering Science 50: 3369-3384.
14. Masud MA, Islam R, Sheikh R, Alam M (2008) High curvature effects on fluid flow through curved pipe with circular cross-section. Proceedings of the 4<sup>th</sup> BSME-ASME International Conference on Thermal Engineering.
15. Nabovati A, Llewellyn EW Sousa ACM (2009) A general model for the permeability of fibrous porous media based on fluid flow simulations using the lattice Boltzmann method. Applied Science and Manufacturing 40: 860-869.
16. Nobari MRH, Amani E (2009) A numerical investigation of developing flow and heat transfer in a curved pipe. International Journal of Numerical Methods for Heat and Fluid Flow 19: 847-873.
17. Park SM (2014) Numerical simulation of core-annular flow in a curved pipe. Master of Science thesis. Delft University of Technology.
18. Petrakis MA, Karahalios GT, Kaplanis S (2009) Steady flow in a curved pipe with circular cross-section. The Open Fuels & Energy Science Journal 2: 20-26.
19. Robey OE (1934) Porous hose irrigation. Michigan Extension Bulletin 133: 1-22.
20. Sobieski W, Trykozko A (2014) Darcy's and Forchheimer's laws in practice. Part 1. The experiment. Technical Sciences 17: 321-335
21. Taylor GI (1929) The criterion for turbulence in curved pipes. Proceedings of the Royal Society of London. Series A, containing papers of a mathematical and physical character 124: 243-249.
22. Verkaik AC (2008) Analysis of velocity profiles in curved tubes. Eindhoven University of Technology, p: 106.
23. White CM (1929) Streamline flow through curved pipes. Proceedings of the Royal Society of London. Series A Containing Papers of a Mathematical and Physical Character 123: 645-663.163.